ACTIVATION OF DOSIMETERS USED IN QA OF MEDICAL LINEAR ACCELERATORS

Kinga Polaczek-Grelik
Department of Medical Physics
University of Silesia, Katowice, Poland
NU-MED Cancer Diagnosis and Treatment Centre Katowice, Poland
kinga.polaczek-grelik@us.edu.pl

Magdalena Nowacka
Department of Medical Physics
University of Silesia, Katowice, Poland

Maciej Raczkowski
Department of Medical Physics
Lower Silesian Centre of Oncology, Wrocław, Poland

ABSTRACT

This paper presents the first results of a project intended to investigate γ-radiation activity induced in dosimeters used in clinical practice during routine quality assurance of high-energy photon beams emitted by electron linear accelerators. Two aspects of the activation via photonuclear reactions (X,n) of therapeutic beam and subsequent capture of secondary neutrons (n,γ) are under considerations: the influence of activation on intrinsic background of the dosimeters and exposure of dosimetrists who operate this equipment. The activation of several types of ionization chambers as well as the silicon diodes was studied after long-time exposure (10 000 MUs) of the 15 MV photon beam (Elekta Synergy). Photon fluxes obtained from spectra of γ-rays registered by HPGe spectrometer were subsequently converted to equivalent doses using appropriate coefficients. The main contribution to the induced activity comes from the neutron capture process on Al, Mn and Cu, therefore it decays quite fast with the half-lives of the order of 15 minutes. Nevertheless, the activation of chlorine was also observed. The estimated equivalent doses to skin and eye lens were in the range 0.19 – 0.62 μSv/min. However, no influence on intrinsic background signal of all studied dosimeters was observed. The preliminary results indicate that induced radioactivity of dosimeters is strongly influenced by therapeutic beam quality and neutron source strength of particular linac. This dependence will be studied deeper in order to quantify it more precisely.

Key Words: **Induced radioactivity, gamma radiation, medical accelerators, ionization chambers, silicon diodes, equivalent doses.**

1. INTRODUCTION

The phenomenon of inducing radioactivity in the construction materials of medical linear accelerators working in high-energy (above ~9MV) photon mode has been widely studied over the last

decades experimentally as well as using the calculations, either a Monte Carlo simulations or the equations of activation and depletion processes, e.g. [1-4]. The induced radioactivity is the consequence of nuclear photo effect (X,n) as well as neutron capture reactions (n,γ), being dependent on linac beam emission time. Therefore, it seems to be especially important during linac commissioning and performance of periodical quality assurance dosimetric tests.

Nuclear photo effect, e.g. (γ/X,n) is observed when energy of photons exceeds approximately 6 MeV in giant dipole resonance (GDR) region. Up to 30 MeV of photon beam generated by linacs, neutrons and protons are the main reaction products [2,5]. However, only neutrons are measured all over the accelerator room [6,7] due to much more limited range of charged particles [4,8].
Computer simulations reported e.g. by Sheikh-Bagheri and Rogers [9] have shown that significant part of high-energy therapeutic photon beam spectrum (up to even 10%) could have energy above the photonuclear reaction threshold for many construction materials, what is exemplary shown in Figure 1.

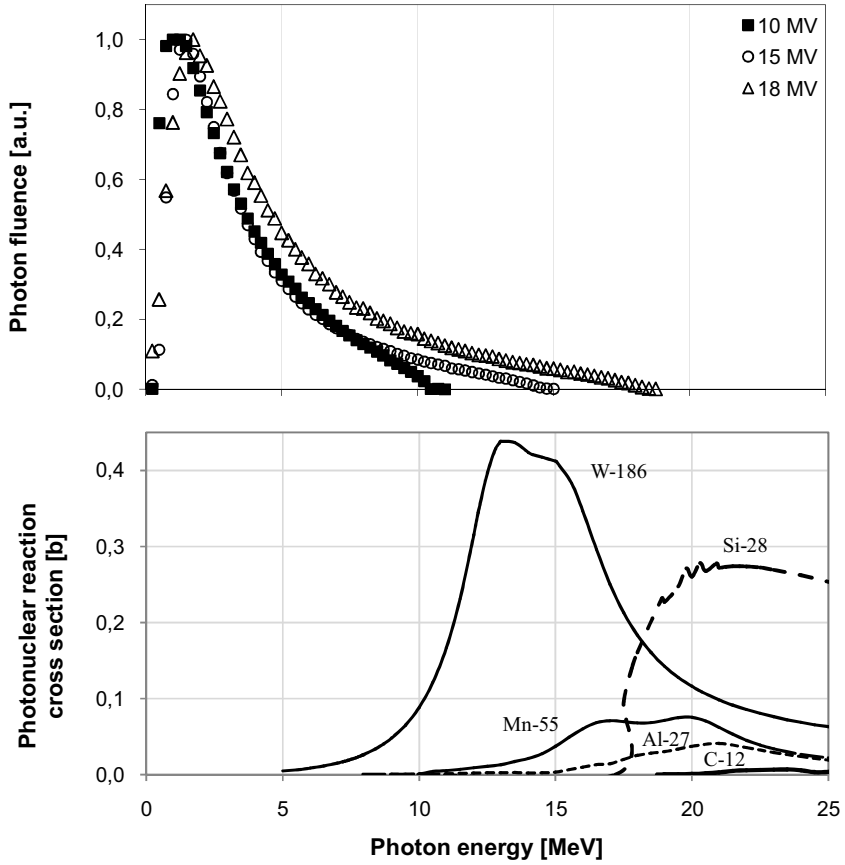

Figure 1. Comparison of the spectra of high-energy therapeutic photon beams generated by linacs obtained in MC simulations by Sheikh-Bagheri and Rogers [9] with the photonuclear reaction cross sections [10] of the most abundant isotopes of the elements found in construction materials of linacs and dosimeters used in clinical practice.

The process of originating radioactivity via photonuclear interaction (γ/X,n) is accompanying by production of secondary particles, mostly – neutrons. The main source of photoneutrons in teleradiotherapy is the accelerator head [1], which is made of heavy materials having lower energy thresholds for this phenomenon. As linac head constitute no shielding against neutrons, these particles are present all over the therapeutic room as it previously has been shown by several authors, e.g. [2,6,7,11] . Moreover, neutron flux can induce radioactivity itself. Cross sections of slow neutron nuclear reactions for many nuclides have high and sharp resonance structure [10]. Generally, the lower neutron energy the higher probability of capture reaction (n,γ). From the in-phantom measurements in QA tests of linac beams point of view, the thermalization process taking place in hydrogen-rich water phantom provides slow neutrons what could gain the activation of dosimeters, e.g. ionization chambers and silicon diodes.

All mechanisms of inducing radioactivity mentioned above can produce unstable isotopes. As a consequence of their decay, secondary gamma radiation is able to appear. The time scale of γ radiation as a consequence of nuclear reactions is directly connected with half-lives of activated radioisotopes. Therefore, it is a process which is extended in time after the end of high-energy beam emission. Consequently, this activity is able to accumulate and finally result in not negligible dose, what is reported for example in [5,12] with respect to patients and workers. However, up to now there is no study concerning the effects of radiation emitted as a consequence of activation of dosimetric equipment, however, some investigations concerning the activation of metal-based ionization chambers were already published, e.g. [13].

The development of modern radiotherapeutic techniques, aimed at improving the conformance of dose distribution in target volume, is usually connected with increased energy emission, e.g. intensity-modulated IMRT techniques or flattening filter-free (FFF) beams. These highly specialized modalities require extended and more sophisticated dosimetric tests to be performed for a given linac before approval for clinical use. During these tests usually beams are emitted for a long time, allowing the induced radioactivity to rise even to the saturation level in the case of short-lived radionuclides.
This paper contains our preliminary results of the study aimed at:

- the assessment of the influence of the activation of commonly used dosimeters on their intrinsic background signal;
- the evaluation of exposure of the staff who use these equipment (hand held carriage, vicinity of eye lens).

2. MATERIALS AND METHODS

Dosimeters commonly used in radiotherapy with external photon beams were investigated in presented study. Among the detectors, characterized in Table 1, were 3 types of ionization chambers as well as silicon diodes dedicated to photon radiation measurements.
The elemental composition of these dosimeters includes mostly non-metals, i.e. C, O, H, F, N, which in general have lower activation cross sections. Nevertheless some of metallic elements are also present, like Al and steel (electrodes), Si (active volume of diodes), W (for homogeneous energy response) and copper wires.

Table 1. Basic characteristics of dosimeters (IBA Dosimetry GmbH) used in presented study.

Type	Model	Active volume [cm^3]	Construction materials	
			Inner electrode	Outer wall
Farmer	FC65-G	0.65	Al	Graphite
Compact	CC13	0.13	C552*	C552*
Compact	CC01	0.01	Steel	C552*
Plane-parallel	PPC05	0.05	PEEK#	C552*
Si diode	PFD^{3G}	0.001	pSi	W, epoxy
Si diode	SFD	0.0004	pSi	epoxy

* C552 – air-equivalent plastic, $\rho = 1.76$ g/cm^3, (2.5% H, 50.2% C, 0.5% O, 46.2% F, 0.4% Si)
# PEEK – Polyether Ether Ketone, $\rho = 1.32$ g/cm^3, type of thermoplastic resins, (C, H, O)

2.1. Experimental Procedure

Activation of dosimetric equipment has been performed in conditions of beam quality assurance tests, i.e. exposition of ionizing chambers and silicon diodes to the treatment X-ray beam and accompanying neutron radiation was performed in the set-up presented in Figure 2, which includes:

- position at central beam axis (CAX),
- irradiation field of $30\times30cm^2$,
- source-to-surface distance (SSD) of 90cm,
- depth of 10 cm in water phantom (48L × 48W × 41H cm^3 of effective scanning volume).

This procedure allowed for taking into considerations real contributions of primary and scattered photons as well as the fast and water-slowed down neutrons in activation process. Since each time whole dosimeter was inside the irradiation field, applying such arrangement one could achieve the maximal activation signal in comparison with partial dosimeter irradiation, i.e. applying lower field size. Each dosimeter was irradiated with the high-energy photon beam with a nominal potential of 15 MV, generated by the Elekta Synergy linear medical accelerator. 10 000 monitor units (MU) with the rate of 600 MU/min was emitted in each case, which means that the activation time was about 17 min.

a)  b) 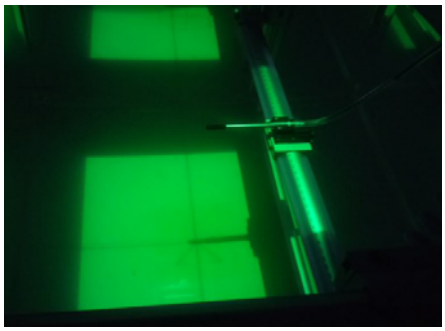

Figure 2. Exemplary view (Farmer-type ionization chamber) of the positioning of dosimeters before activation: a) general view with water phantom and linac head visibility, b) in-field positioning with respect to CAX.

2.2. Intrinsic Signal

The instrumentation issue of presented study has been focused on monitoring of dosimeters' intrinsic charge signal, to check whether should it be periodically compensated during long-time measurements.
The background signal of each dosimeter (in nC) has been investigated before the irradiation as well as immediately after the end of beam emission.
Charge signal of each ionization chamber was determined with the use of a standard electrometer (Dose1, IBA Dosimetry), whereas in case of silicon diodes CCU unit coupled with OmniPro Accept7 software (IBA Dosimetry) was used.
Before the irradiation 10-second measurement was repeated 10 times, then averaged and referred as intrinsic background signal. After the end of activation procedure, 10 second-lasting measurements of the charge were carried out for one hour, to investigate potentially occurring decay of intrinsic signal connected with the activated radionuclides.

2.3. Induced Radioactivity

The induced radioactivity of each studied dosimeter has been investigated using gamma spectrometry system consists of:

- portable coaxial high-purity Ge detector with reverse electrodes (REGe) (Canberra Inc.);
- multichannel analyser InSpector 2000 (8194 channels);
- Genie2000 software, v.3.2.1.

The gamma-energy spectrum in the energy range of 6-3150 keV of each studied dosimeter has been registered twice:

1) before the activation process, for 30 minutes and
2) immediately after the end of irradiation, for one hour.

The first spectrum is considered as an internal background of the investigated equipment (containing also the natural radiation of the place in which the measurements were carried out). The second spectrum was analyzed in terms of induced radionuclides.
The set-up for induced radioactivity registration is presented in Figure 3.

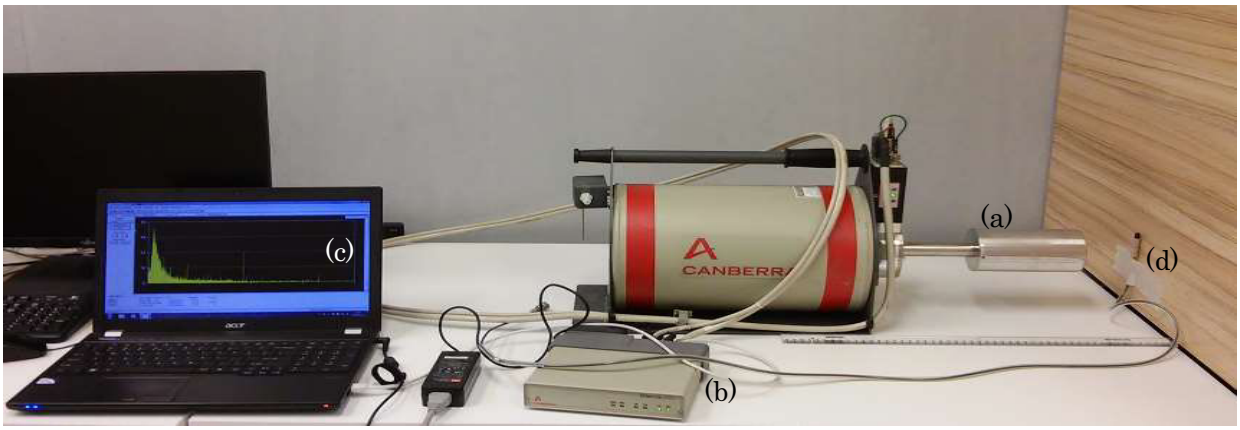

Figure 3. Spectrometric system, which contain REGe detector (a), multichannel analyzer (b), registration software (c) in arrangement with activated ionization chamber (d) during induced radioactivity measurement.

2.3.1. Spectrometric analysis

The spectrometric analysis of radionuclides has been shown by us previously [14] to be good method of low dose assessment in comparison with the standard dose rate meters, giving furthermore the additional information of the elements, which are the most intense sources induced radiatoactivity and secondary doses.
Identification of radionuclides was done on the base of the energy at the centre of photopeak, therefore, this method required exact energy calibration of spectrometric system. This calibration was performed with the use of point-like sources (^{22}Na, ^{54}Mn, ^{57}Co, ^{60}Co, ^{65}Zn, ^{109}Cd, ^{133}Ba and ^{137}Cs) with the activity of the order of 1 μCi (comparable with experimental once), which energies covered most of the useful energy range.

The quantitative analysis of gamma radiation flux (required for dose estimation) at a distance of 10 cm from the dosimeters was based on net count rate under the photopeak around the energy of photons emitted by particular radioactive nuclide (E_γ). The efficiency (ε) calibration of spectrometric system is described by the Equation (1).

$$\varepsilon = 4.74 \cdot E_{\gamma}^{-1.05} \cdot \exp\left[-\left(\frac{E_{\gamma}}{-0.63} \right)^{132.27} \right] \quad (1)$$

2.3.2. Dose calculation

Equivalent doses to skin and eye lens were estimated on the base of the gamma-ray flux of particular energies obtained from registered spectra, applying fluence-to-dose conversion coefficients according to ICRP report no 74 [15]. Since this report supplies conversion coefficients for discrete values of energies, according to the suggestions given therein, values required in our analysis were calculated using Lagrange interpolation formula of 3rd degree (4-point). The dependency of conversion coefficients on photon energy is exemplary shown in Figure 4.

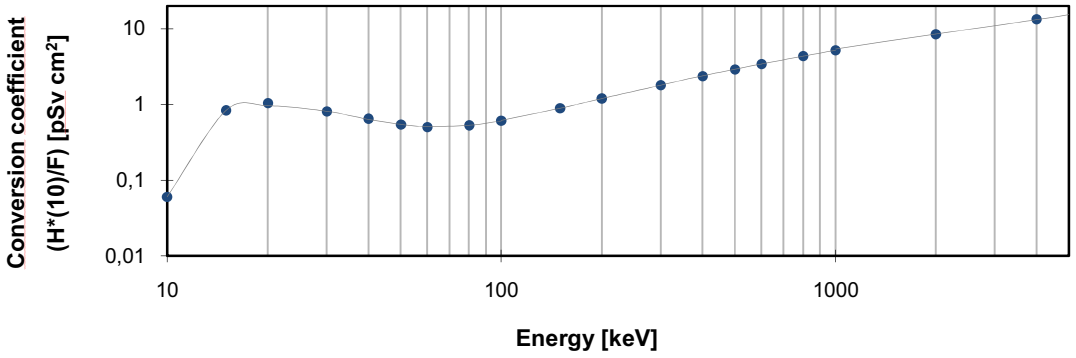

Figure 4. Photon fluence-to-quivalent dose conversion coefficients obtained on the base of [15]. The points indicate discrete values given in [15], which serves for interpolation with the use of Lagrange interpolation formula.

2.3.3. Uncertainty of the method

The major source of the uncertainty in applied technique is the statistical error of gamma-ray counting performed by spectrometry system. This contribution to the total uncertainty may be reduced by applying longer irradiation time, allowing to reach the saturation activity for majority of nuclides. In applied activation and spectrum registration time conditions this results in average counting uncertainty of 10 %.
The discrepancies in conversion coefficient values specified in report 74 of ICRP [15] of 10% are another source of total dose uncertainty.
Additional uncertainty in determination of the activity, and afterwards in estimation of photon flux and subsequently – equivalent doses, could appear due to the use of point sources in calibration process, whereas extended volume sources were under study. However, as our previous measurements for higher activity level have shown [14], the results obtained using presented method in comparison with the use of a standard dose rate meter agree within the accuracy of 4 %.

3. RESULTS

3.1. Dosimeters Reading

Typical values of intrinsic background current signal for studied ionization chambers with applied operation voltage of 300V is 0.0010 ± 0.0004 nC. The leakage current of silicon diodes under investigation is 0.0040 ± 0.0008 nC. These values were obtained as an average from 10 consecutive measurements before irradiation.
Activation process of ionization chambers does not increase the intrinsic charge signal (average value is around 0.0008 ± 0.0003 nC), i.e. it remains statistically dispersed over time, what is presented exemplary in Figure 5. In case of silicon diodes the signal was increased about 3 times to the value of 0.011 ± 0.001 nC. Even after 10 minutes from the end of irradiation the background current signal for diodes was still rising (see Figure 6), what suggests that it was not affected by decay of activated nuclides.

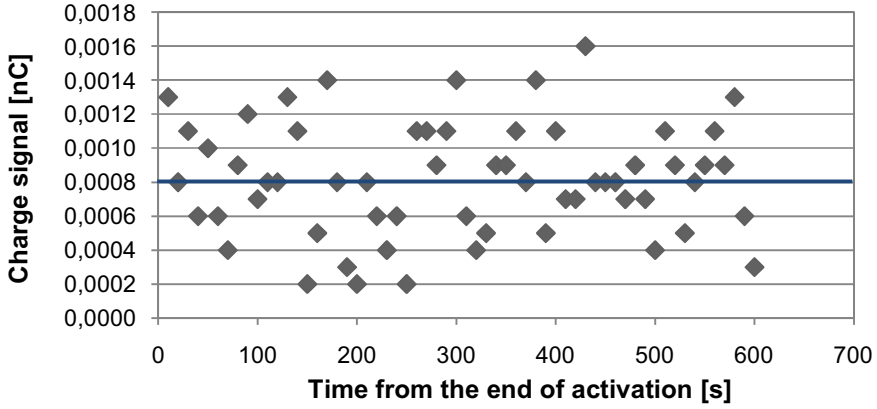

Figure 5. Charge signal of CC01 ionization chamber after irradiation with 10 000 MUs 15MV photon beam. The blue line represents the average signal.

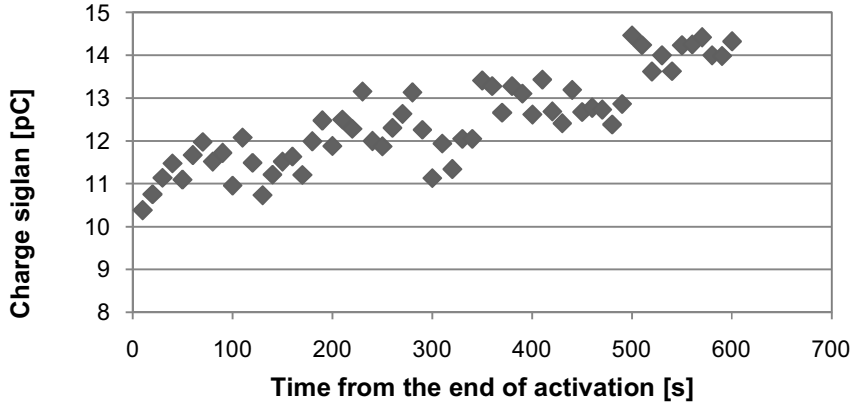

Figure 6. Evolution in time of charge signal for silicon diode irradiated with 10 000 MUs 15MV photon beam.

3.2. Activated Radionuclides

The identification of activated radionuclides (presented in Table 2) has been done using the spectra of activated dosimeters registered for one hour after irradiation, to achieve good counting statistics.

Table 2. Gamma energy-ordered analysis of activation process occurring in studied dosimeters during the irradiation with 15 MV therapeutic photon beam.

Radionuclide origin	Energy of γ-ray [keV]	Half-life $T_{1/2}$	Dosimeter
$^{186}W(n,\gamma)^{187}W$	479.5	23.7 h	PFD
$^{186}W(n,\gamma)^{187}W$	551.5	23.7 h	PFD
$^{186}W(n,\gamma)^{187}W$	618.4	23.7 h	PFD
$^{186}W(n,\gamma)^{187}W$	685.8	23.7 h	PFD
$^{186}W(n,\gamma)^{187}W$	772.9	23.7 h	PFD
$^{55}Mn(\gamma/X,n)^{54}Mn$	834.9	312.1 d	CC01
$^{55}Mn(n,\gamma)^{56}Mn$	846.8	2.6 h	CC01, CC13, FC65-G, SFD, PFD
$^{65}Cu(n,\gamma)^{66}Cu$	1039.3	5.1 min	CC01, CC13, FC65-G, PPC05, SFD, PFD
$^{59}Co(n,\gamma)^{60}Co$	1173.2	5.3 y	CC01
$^{58}Fe(n,\gamma)^{59}Fe$	1291.6	44.5 d	CC01
$^{59}Co(n,\gamma)^{60}Co$	1332.5	5.3 y	CC01
$^{65}Cu(\gamma/X,n)^{64}Cu$	1345.8	12.7 h	CC01, FC65-G
$^{37}Cl(n,\gamma)^{38}Cl$	1642.7	37.2 min	CC01, CC13, FC65-G
$^{27}Al(n,\gamma)^{28}Al$	1779.0	2.2 min	FC65-G, PPC05
$^{55}Mn(n,\gamma)^{56}Mn$	1810.8	2.6 h	CC01, FC65-G, SFD, PFD
$^{55}Mn(n,\gamma)^{56}Mn$	2113.1	2.6 h	CC01, PFD
$^{37}Cl(n,\gamma)^{38}Cl$	2167.4	37.2 min	CC01, CC13, FC65-G, PPC05, SFD, PFD

The analysis presented in Table 2 has shown, that in case of compact chamber CC01 and Farmer-type chamber FC-65G, the most intense activation occurs in the materials of inner electrodes, i.e. stainless steel (Fe, Mn, Co) and aluminium, respectively. In case of shielded photon diode PFD, material (W) aimed at making the response uniform over all photon energies, is the most susceptible on activation process. In all plastic materials activation concerns only chlorine in applied experimental conditions (15MV beam). This could be different for higher therapeutic beam energies and/or more intense neutron fluxes, i.e. linacs from other manufacturers. Copper wires connected with all studied dosimeters are also activated.

The exemplary comparison of the spectra registered before and after 15 MV photon beam irradiation, during which the activation occurs is shown in Figure 7. It shows that the studied effects are clearly visible only for radionuclides which were able to reach the saturation activity during irradiation, i.e. short-lived once (e.g. ^{28}Al and ^{66}Cu).

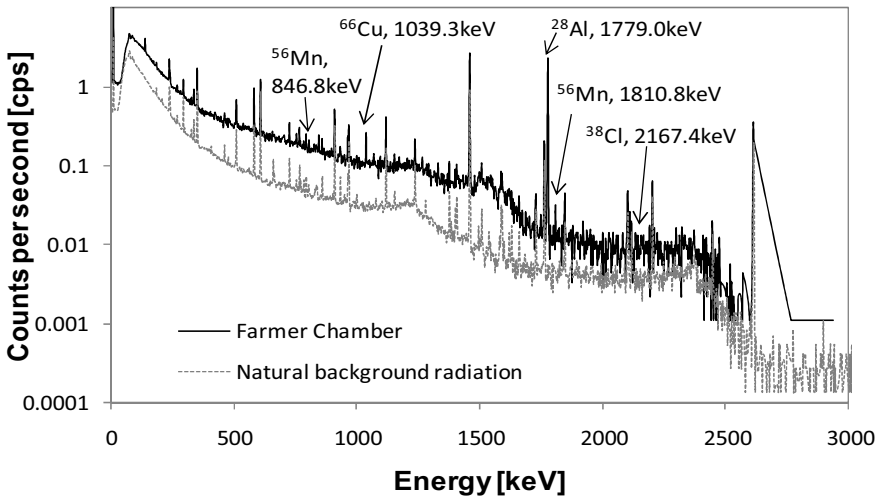

Figure 7. Spectra of gamma radiation of activated Farmer-type ionization chamber FC-65G (solid line) and natural background radiation (dotted line) for comparison.

3.3. Equivalent Doses

Equivalent doses to skin and eye lens were calculated due to higher risk for these organs during operation of dosimetric equipment in teleradiotherapy. The results are presented in Table 3. Since the limited time of direct contact with this equipment as well as the fact, that the most activated radionuclides are short-lived, i.e. ^{28}Al ($T_{1/2}$ = 2.2 min) and ^{37}Cl ($T_{1/2}$ = 37.2 min), the doses are expressed in μSv/min. The estimated values are relevant for the distance from radiation source to the skin/eye lens of 10 cm, since in such conditions the detection efficiency curve was determined.

Table 3. Equivalent doses to skin and eye lens, dominant components of these doses and effective half-lives estimated on the base of registered gamma-energy spectra of activated dosimeters.

Dosimeter	Equivalent dose [μSv/min]		Dominant component	Second contributor	Effective half-life [min]
	Skin	Eye lens			
FC65-G	0.38 ± 0.06	0.41 ± 0.08	$^{37}Cl(n,\gamma)^{38}Cl$	$^{27}Al(\gamma/X,n)^{26}Al$	16 ± 3
CC13	0.22 ± 0.05	0.24 ± 0.05	$^{37}Cl(n,\gamma)^{38}Cl$	$^{55}Mn(n,\gamma)^{56}Mn$	12 ± 2
CC01	0.56 ± 0.13	0.62 ± 0.13	$^{55}Mn(n,\gamma)^{56}Mn$	$^{37}Cl(n,\gamma)^{38}Cl$	16 ± 3
PPC05	0.19 ± 0.04	0.20 ± 0.04	$^{37}Cl(n,\gamma)^{38}Cl$	$^{27}Al(n,\gamma)^{28}Al$	19 ± 4
PFD^{3G}	0.37 ± 0.10	0.41 ± 0.10	$^{55}Mn(n,\gamma)^{56}Mn$	$^{37}Cl(n,\gamma)^{38}Cl$	16 ± 3
SFD	0.22 ± 0.05	0.24 ± 0.05	$^{37}Cl(n,\gamma)^{38}Cl$	$^{27}Al(\gamma/X,n)^{26}Al$	12 ± 2

4. SUMMARY AND CONCLUSIONS

Presented study have shown that the process of radionuclides activation takes place in materials of commonly used dosimeters, e.g. ionization chambers and silicon diodes, at a measurable level. However, it has been shown that this induced activity does not affect the intrinsic signal of these dosimeters. Therefore, it seems to be unnecessary to periodically compensate the background signal during the performance of long-lasting medical linac commissioning or QA tests for that reason. Nevertheless, in case of silicon diodes, typical behavior of this type of dosimeters was demonstrated, i.e. the intrinsic signal increases rapidly with collected dose, which should be keeping in mind by dosimetrists.

The analysis of gamma-energy spectra of activated dosimeters have shown, that in this case neutron capture (n,γ) process is the main mechanism of inducing radioactivity. Radionuclides originated this way are rather short-lived, what has been pointed out by the assessment of effective half-lives of apparent radioactivity induced in each dosimeter under study, being of the order of 15 minutes. Furthermore, since intensity of neutron production depends on therapeutic beam end-point energy and linac construction (manufacturer), the studied phenomenon is beam-quality dependent, and is currently the subject of ongoing research project.
As suggested by the overview of photonuclear reaction cross sections (see Figure 1), silicon in diodes undergoes no activation in the 15 MV therapeutic beam. Nevertheless, applying higher voltage, the results could be different.

Skin of hands and eye lens – organs which are the most likely to be exposed to radiation during the operation and in-phantom positioning of dosimeters, are able to receive equivalent doses of the order of a tenth of μSv/min, in which the activation of chlorine and inner electrode material contribute the most. It is worth noticing that such an exposition is usually not detected by the personal dosimeters worn by the staff, which are calibrated in personal dose equivalent $H_p(10)$.

ACKNOWLEDGMENTS

The study was partially support by the program for young scientists (KPG) realized in the Institute of Physics, University of Silesia also aimed at supporting the cooperation with business sector.

REFERENCES

[1] J. Becker, E. Brunckhorst, R. Schmidt, "Photoneutron production of a Siemens Primus linear accelerator studied by Monte Carlo methods and a paired magnesium and boron coated magnesium ionization chamber system", *Physics in Medicine and Biology,* **52(21),** pp.6375 – 6387. (2007)
[2] H.W. Fisher, B.E. Tabot, B. Poppe, "Activation process in medical linear accelerators and spatial distribution of activation products", *Physics in Medicine and Biology*, **51**, pp. N461 – N466. (2006)
[3] K. Polaczek-Grelik, B. Karaczyn, A. Konefał, "Nuclear reactions in linear medical accelerators and their exposure consequences", *Applied Radiation and Isotopes*, **70**, pp. 2332 – 2339. (2012)
[4] W. Abdel-Rahman, E.B. Podgorsak, "Neutron-activation revisited: the depletion and depleteon-activation models", *Medical Physics*, **32(2)**, pp. 326 – 336. (2005)
[5] I. Gudowska, A. Brahme, P. Andreo, W. Gudowski, J. Kierkegaard, "Calculation of absorbed dose and biological effectiveness from photonuclear reactions in a bremsstrahlung beam of end point 50 MeV", *Physics in Medicine and Biology*, **44**, pp. 2099 – 2125. (1999)
[6] J.-P. Lin, T.-Ch. Chu, S-Y. Lin, M.-T. Liu, "The measurement of photoneutron in the vicinity of Siemens Primus linear accelerator", *Applied Radiation and Isotopes*, **55**, pp. 315 – 321. (2001)
[7] A. Konefał, A. Orlef, M. Dybek, Z. Maniakowski, K. Polaczek-Grelik, W. Zipper, „Correlation between radioactivity induced insi de the treatment room and the undesirable thermal/resonance neutron radiation produced by linac", *Physica Medica*, **24**, pp. 212 – 218. (2008)
[8] P.D. Allen, A. M. Chaudhri, " Charged photoparticle production in tissue during radiotherapy", *Medical Physics*, **24**, pp. 837 – 839. (1997)
[9] D. Sheikh-Bagheri, D.W.O. Rogers, "Monte Carlo calculations of nine megavoltage photon beam spectra using the BEAM code", *Medical Physics*, **29**, pp. 391 – 402. (2002)
[10] ENDF/B-VII.1 (USA, 2011) data base, available online. URL http://www.nndc.bnl.gov/sigma/search.jsp (2016)
[11] K. Polaczek-Grelik, B. Karaczyn, M. Grządziel, M. Pieńkos, A. Konefał, W. Zipper, „The map of thermal and resonance neutron distribution insi de the treatment room for akcelerator therapy", *Polish Journal of Environmental Studies, Series of Monographs*, **1**, pp. 139 – 145. (2010)
[12] L. L. Donadille et al., "Radiation protection of workers associated with secondary neutrons produced by medical linear accelerators", *Radiation Measurements*, **43**, pp. 939 – 943. (2008)
[13] Y.-H. Liu et al., "The activation contamination in the metal-based ionization chambers as gamma dosimeters in the mixed field dosimetry", *Radiation Measurements*, **45**, pp. 1427 – 1431. (2010)
[14] M. Janiszewska, K. Polaczek-Grelik, M. Raczkowski, B. Szfron, A. Konefał, W. Zipper, „Secondary radiation dose during high-energy total body irradiation", *Strahlentherapie und Onkologie*, **190(5)**, pp. 459 – 466. (2014)
[15] H. Smith (ed.), *Conversion coefficients for use in radiological protection against external radiation*, ICRP Publication 74, Pergamon Press, Oxford, United Kingdom, (1996)